Model and Control design of All-electric Quadcopter

Unmanned Aerial Vehicles such as Quadcopters are becoming very popular for military, surveillance, inspection, as well as large-scale disaster management, and supply delivery applications. The most notable shortcoming of the current generation of such vehicles is the limited flight time.

This problem could be attributed to the power source limitations. Hydrogen fuel cells are very promising with relatively high energy density and yet environmentally friendly source of energy. The fuel cell can be coupled with a battery like a Li-ion based to form a hybrid power unit that can achieve clean and dependable energy source for continuous operation of a quadcopter.

In this study, the flight time can be considerably increased by utilizing an on-board dynamic model-based control architecture, which controls the power supply parameters of the vehicle for optimal operation at high efficiency. The simulation and characterization of the proposed control architecture is presented in this study. In this project, the fuel cell and battery are modeled as separate primary power sources for the quadcopter while the four motors that run the propeller of the quadcopter are modeled as primary power sinks. The model is simulated for various flight conditions including steady hover and lift off using Simscape to determine the power demand and angular velocity of each motor.

Based on the open-loop responses, a classical PID control algorithm should be developed to increase flight operation time. You may use as many conventional PID controllers as needed in any arrangement that is practical and efficient. **Objectives:**

- *Complete models of the polymer electrolyte membrane fuel cell or battery, quadcopter motors and peripheral parts (as appropriate) in MATLAB & Simulink where a power system of a battery or a fuel cell will power continuous operation of an UAV.*
- *Integrate the power system with Quadcopter components such as the motors in Simulink/SimMechanics to simulate the performance.*
- *Analyze the open loop response for lift off and landing.*
- *Identify appropriate variables and compute parameters in MATLAB & Simulink for control design.*
- *Develop a PID controller strategy to ensure reliable system performance.*
- *Evaluate the closed-loop response of the system.*

For further background on the project and to understand the MATLAB/Simulink/SimMechanics files provided, please see the report included in **Appendix B** For grading criteria and report guidelines see **Appendix A**.

APPENDIX A

A.1 Simulation Report – Grading Rubric

Full report:	Abstract	1 points
	Introduction	1
	Modeling Approach	2
	Open Loop Results	2
	Closed Loop Results	2
	Discussion/Conclusion	2
	References	1
	Appendix	1
	Completeness, creativity, and professional quality appearance	3 points

Bonus problem (Appendix) – 2 pts

Develop the frequency response model in MATLAB for your report:

1. Bode plot of Open-loop step response
2. Gain and Phase Margin

Introduction

The purpose of technical writing is to communicate technical information as clearly and effectively as possible. You should not use language that is excessive or complex. This is typically achieved by writing at an 8th grade level. This does not mean you have to dumb down your engineering. Define terminology that might be confusing, avoid wordiness, and avoid jargon. Don't be dramatic; drama is used in creative writing to elicit an emotional response. Technical writing is centered on the use of logic.

General Format Issues

- The Interim and Final Reports must be of professional quality, and entirely computer generated.
- Each Interim report can be submitted in Blackboard or email to faculty mentor.
- The Final signed report must be submitted in Blackboard or email to faculty mentor.
- A 30 page maximum length is *suggested*, excluding Appendices and cover sheet.

Margins: Set your margins as indicated below for the entire manuscript.

Top: 1 inch Right: 1 inch
Bottom: 1 inch Left: 1¼ (one and one-quarter) inch

Margins should be justified to give a professional appearance

Fonts: Use Times New Roman or Arial fonts. You must be consistent in using the font you choose throughout the entire Final Report.

Font Size: 10-12 point regular
Exception: Footnotes and entries within a table/figure may be as small as 8 point. 14 point is acceptable for major headings. Consistency in use of font size is essential.

Font Style: Use italics in place of underlining throughout the manuscript.
Do not use bold fonts except for headings and when required as part of a formula.

Corrections: Only a clear print copy is acceptable. Corrections made by hand or using correction fluid or correction tape are unacceptable.

Spacing: Text must be 1.5 spaced or double-spaced, but be consistent with your choice. Single space and indent block quotes and numbered lists. Preferred paragraph indentation is one-half inch (5 to 7 spaces).

Grammar: Good grammar and spelling are essential.

Voice: The report can be written in either passive ("a concept was selected") or active ("we selected a concept") voice. Pick whichever sounds more natural and use it predominantly. However, do not use the passive voice exclusively. Doing so can lead to wordy and highly convoluted sentences.

Use the passive voice to change the order of information in a sentence, to vary the sentence structure for variety's sake, or to eliminate the true subject if it is not important. Typically, passive sentences use more words to express an idea.

Tense: Use past tense to describe what you did or found out. For example, "We built and tested a prototype." Use present tense to describe things that were known before your project. For example, "Squirrels are warm-blooded."

Use future tense to describe what has not yet been done but what will be done. The present and future tenses may be used in the interim reports.

Headings and Sub-Headings:

Left justify section titles. Use the same numbering as shown in the Organization sections.

Divide your information up into small, manageable chunks. Use headings and subheadings to categorize the information so people can easily find it. You should have at least one heading on each page.

Pagination: Center page numbers at the bottom of the page. Use the same font and size as the text (check auto-numbering to ensure proper sizing). Page numbers should appear one-half to one inch from the edge of the paper. Do not use sub-numbers or alpha-numeric values such as 34-A or 76.1 to indicate manuscript pages.

Preliminary Pages:

Number the Table of Contents, List of Tables, and List of Figures pages in lower case Roman numerals (i, ii, iii, etc.) in the same font and size as the rest of the text. The first numbered page (i) is the Table of Contents. Do not place a page number on the Title Page or Executive Summary.

Text: Beginning with the first page of the text (Section I), number pages consecutively with Arabic numerals (starting with the number "1") through the last page of Section VIII, including full-page tables, figures, and all other illustrations lying therein. Number each appendix separately, with the page number preceded by the appendix letter (e.g., A1,

APPENDIX B

Introduction

Investments have been increasing for the purpose of utilizing electrical propulsion unmanned aircraft systems (UAS) in many areas such as reporting weather, package delivery, land surveying, and military missions. Whether it is indoor or outdoor, an UAS that is designed and built for its respective environment applications can provide a tremendous amount of advantages in terms of safety, efficiency, reliability [16], ease of control, and minimal disturbances to its environment. The main problem concerning an electrical propulsion UAS is its underwhelming flight duration using conventional batteries [7,8], compared to larger flight systems that relies on carbon-based fuels. In this article, a fuel-cell based power system connected to a battery has been studied to improve this aspect of UAS. Many tests have been taken to see the effects of fuel-cell incorporated into aircrafts [9-16]. Results could be promising due to high energy density provided by hydrogen fuel cells, which leads to longer mission endurance [17-20].

Depending on the mission objectives, the types of UAS may vary. An UAS, such as a quadcopter, is sufficient for many engineering applications in which the mission requires the need to carry a specific load at a steady motion and the ease of control in much smaller environments, compared to a plane which requires a much larger environment for take-off and landing as well as an increase in complexity in controls due to aerodynamics of the wings. Construction companies have started to use drones to keep track of their progress on the job site by staying stationary or flying out a few miles and capture progress being made on site [21]. A fuel-cell and battery hybrid power system, in which the battery acts as a boost, such as a large capacitor, may be beneficial for quadcopter missions that require a large power surge for short flight durations and a fast response to load fluctuations in power demand [5, 15].

Although hybridization may not be a necessity [22], the higher power density of a battery compared with a fuel-cell system may lead to a lower overall weight if peak power is only required for a short period of time and cruise power is significantly lower than the peak power demand. A hybrid system can additionally assist with accommodating rapid load changes as a fuel cell's response to load changes is usually restricted by the need to avoid membrane damage caused by fuel or oxygen starvation [23-25]. Hybridization can also lower the capital cost of the system, reduce its mass and volume, and result in improved system efficiency [18-20].

This article provides a system evaluation through software such as MATLAB and Simulink® by designing virtual simulations based on mathematical equations governing the fuel cell. A control (such as PI or PID) will be implemented and experimented for the fuel cell as well as for the motor model. The models for the fuel cell and the motors will then be combined and tested simultaneously. Simscape® by Mathworks®, Inc., [36] may be used to provide a visual aid in terms of the mechanical behavior of the quadcopter. Finally, data obtained will be evaluated and compared to literature.

Fuel cell

Modeling Approach

The mathematical model of the fuel cell voltage output along with its controls will be analyzed. The selected fuel cell for this experiment is Horizon H-200. The simulation was done by using Simulink®. The power of the proton exchange membrane fuel cell (PEMFC) is generated by the electrochemical reactions. The output voltage of V_{cell} of the fuel cell is given by [26].

$$V_{cell} = E_{Nernst} - V_{act} - V_{ohm} - V_{conc} \quad (1)$$

where E_{Nernst} is the Nernst voltage which depends on the cell temperature T_{st}, hydrogen partial pressure P_{H2}, and oxygen partial pressure P_{O2}, which can be calculated by

$$E_{Nernst} = 1.229 - 0.85 \times 10^{-3}(T_{st} - 298.15) + 4.3085 \times 10^{-5}\left[\ln(P_{H2}) + \frac{1}{2}\ln(P_{O2})\right] \quad (2)$$

The activation voltage V_{act} at the anode and cathode side is

$$V_{act} = -[\xi_1 + \xi_2 * T_{st} + \xi_3 * T_{st}\ln(Co_2) + \xi_4 * T_{st}\ln(i_{FC})] \quad (3)$$

where ξ_i(i = 1, 2, 3, 4) are the fitting coefficients, i_{FC} is the stack current, and C_{O2} is the concentration of oxygen that is denoted by [27].

$$C_O{}_2 = \frac{O}{5.08*10^6 \exp\left(\frac{498}{T_{st}}\right)} P{}_2 \quad (4)$$

The ohmic voltage loss V_{ohm} is

$$V_{ohm} = i_{FC}(R_M + R_C) \quad (5)$$

where R_c is a constant value, R_M is the equivalent resistance of the membrane given by

$$R_M = \frac{(\rho_M * l)}{A} \quad (6)$$

in which the specific resistivity ρ_M is [27]

$$\rho^{M} = \frac{181.6\left[1+0.03*\left(\frac{i_{FC}}{A}\right)+0.062\left(\frac{T_{st}}{303}\right)\left(\frac{i_{FC}}{A}\right)^{2.5}\right]_2}{[\lambda_M - 0.634 - 3(\frac{i_{FC}}{A})] \exp[4.18(1-\frac{303}{T_{st}})]} \tag{7}$$

where l and A represent the thickness of the membrane and cell active area, respectively. λ_M is the average water content in the membrane [27-28].

The concentration voltage drop V_{conc}, is expressed by reference [28].

$$V_{conc} = -\frac{RT_{st}}{2F}\ln\left(1-\frac{j}{j_{max}}\right) \tag{8}$$

where j is the current density defined by $j = i_{FC}/A$.

The transient dynamics of PEMFC has been modeled by many studies. This paper utilizes the variable double-layer equivalent circuit to simulate the electrochemical transient phenomenon of the PEMFC [28,29], where the variable capacitance is calculated by

$$C_{act} = \frac{1}{\xi_5 R_{act}} \tag{9}$$

where ξ_5 is the constant value, R_{act} is the activation polarization resistance that is denoted by

$$R_{act} = \frac{V_{act}}{i_{FC}} \tag{10}$$

The activation overvoltage V_{act}, is substituted by the capacitor voltage V_C, which is defined by

$$\frac{dV_C}{dt} = \frac{1}{C_{act}}\left(i_{FC} - \frac{V_{act}}{R_C}\right) \tag{11}$$

The cell dynamic model can be expressed in

$$V_{cell} = E_{Nernst} - V_C - V_{ohm} - V_{conc} \quad (12)$$

The stack output voltage V_{FC} is obtained by

$$V_{FC} = N * V_{cell} \quad (13)$$

N represents number of stacks. The equations are modeled in MATLAB as block diagrams using SIMULINK shown in Fig. 1.

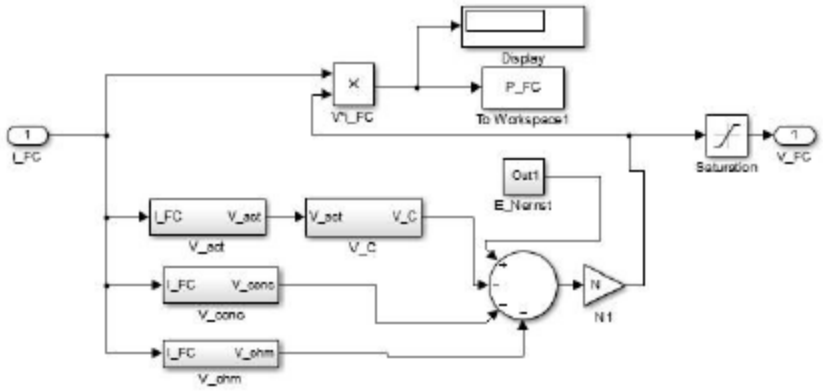

Fig. 1 – Block diagram of PEMFC on MATLAB/SIMULINK

The simulation (by testing Horizon H-200 PEMFC) results of PEMFC polarization and power curve using Simulink® block diagram from Fig. 1 is shown in Fig. 2. Compared to literature, the results indicate that the model is accurate [34].

Table 1. PEMFC model parameters.

Parameter	Value
T_{st}	$333.15\ K$
P_{H2}	$2\ atm$
P_{O2}	$0.21\ atm$
$\xi_1, \xi_2, \xi_3, \xi_4, \xi_5$	$-1.09, 3.48x10^{-3}, 5.8x10^{-5}, 9x10^{-5}, 20$
R_C	$2.05x10^{-2}\ \Omega$

l	$0.0178\ cm$
A	$22.5\ cm^2$
λ_M	11
R	$8.3145 \frac{J}{mol * K}$
F	$96{,}485 \frac{C}{mol}$
j_{max}	$0.622 \frac{A}{cm^2}$
N	40

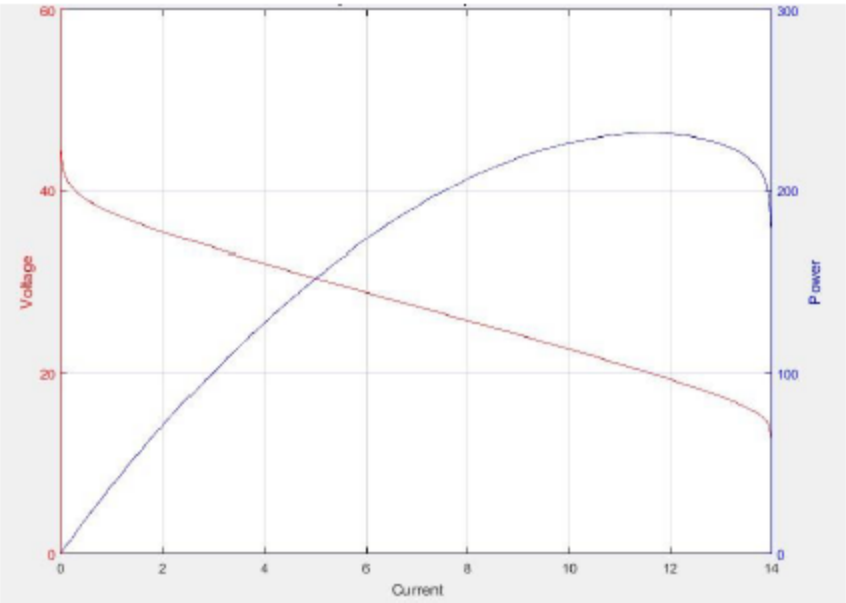

Fig. 2 - PEMFC polarization and power curve.

Control Approach

A controller was necessary to operate the flowrate of hydrogen feed into the fuel cell. Based on the mechanics of the hydrogen tank, a PI controller was implemented over PID [37]. A Simulink block diagram is shown in Fig. 3 for the PI loop of PEMFC.

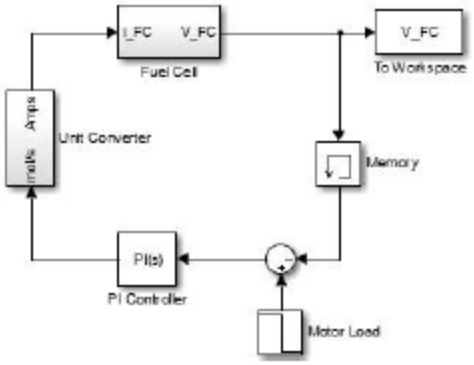

Fig. 3 – PI control of PEMFC

The step function block represents motor load which ranges from 48 to 20 volts. The motor's load, along with V_{FC}, goes into a junction to produce an error that will feed into the PI block. The output from the PI control (in mols/s) is then converted to current in A to be fed into the fuel cell using the correlation from Ref. [30].

$$n_{H2} = \frac{IN}{2F} \tag{14}$$

where n_{H2} is in mol/s of hydrogen flowrate, $I = i_{FC}$, and F is Faraday's constant. By calculating the difference between the load from the motors as well as feedback from the fuel cell, the error can be obtained. This error will then be fed into the controller. Using the error, the PI controller adjusts the valve which opens the tank, this will result in either increasing or decreasing the flowrate. The Memory block between the junction and fuel cell output holds and delays its input by one major integration time step. The output of tuned PI controller is shown in Fig. 4. The step response of V_{FC} from 48 V approaches steady state, which is approximately 20 V. The rise-time is approximately 1.8 sec while overshoot being less than 5% of the entire range which makes it acceptable. Steady-state error being less than 1% can be negligible. The output V_{FC} has a steady-state error of 20.005 ± 0.025 V. For 6.69 mol of hydrogen, the fuel cell can operate at an input of i_{FC} = 7 A (1.451×10^{3} mol/s) for approximately 77 minutes.

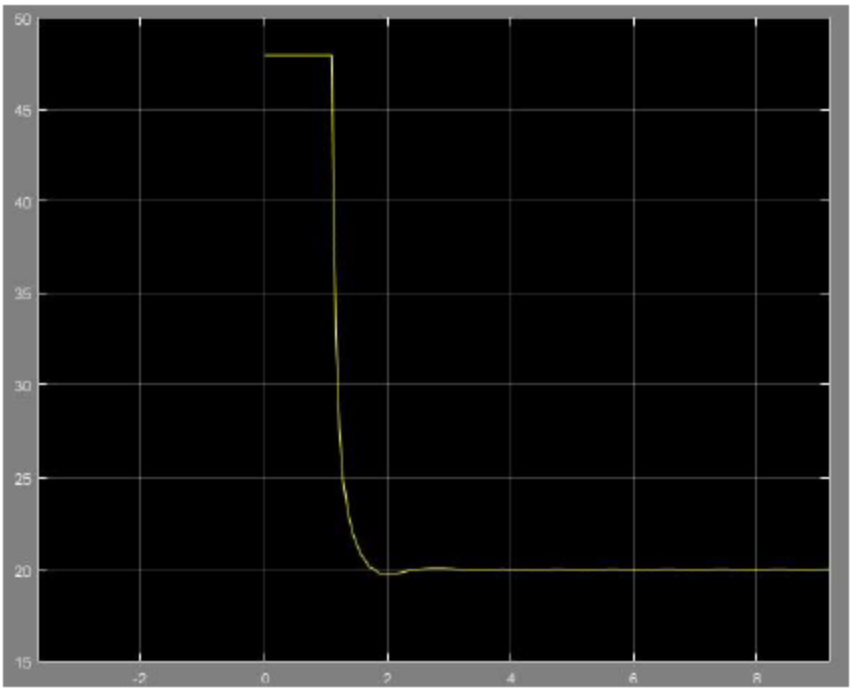

Fig. 4 – Voltage output from fuel cell

Motor Modeling and Specifications Modeling and control of quadcopter motors

The analysis reported in this paper on a T-Motor® model MIT 2826. It is a DC brushless motor with parameters that were measured using the process described in [31]. The quadcopter design required four (4) of these engines. They are designed to work independently from each other and can be adjusted individually to match the power fly requirement.

Physical set up of the T-Motor®

From reference [2] a detail design and parts specification are provided. Those specification are necessary in determining the physical parameter of the motor.

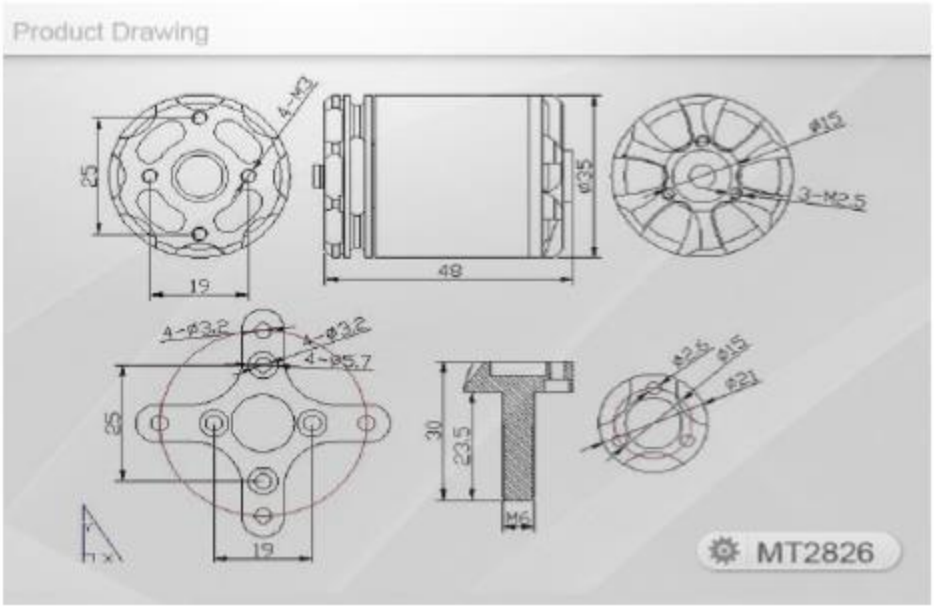

Fig. 5 - MT2826 Motor drawing

TABLE 2 - MT2826 MOTOR SPECIFICATION

Specifications:	
KV	550
Configu ration	12N14P
Stator Diameter	28mm
Stator Length	26mm
Shaft Diameter	5mm
Motor Dimensions(Dia.*Len)	Φ35×48mm
Weight (g)	187g Idle

current(10)@10v(A).....0.9A No.of Cells(Lipo).....3-6S
Max Continuous current(A)180S.....35A
Max Continuous Power(W)180S.....700W
Max. efficiency current.....(10-28A)>83%
internal resistance.....42mΩ

Table 3 - MT2826 Detail Motor Specifications

Item No.	Volts (V)	Prop	Throttle	Amps (A)	Watts (W)	Thrust (g)	RPM	Efficiency (g/W)	Operating temperature(℃)
MT2826 KV550	14.8	T-MOTOR 12*4CF	50%	3.9	58	500	5000	8.66	42
			65%	5.2	77	630	5500	8.19	
			75%	6.2	92	700	5900	7.63	
			85%	8.2	121	870	6550	7.17	
			100%	10	148	1020	7000	6.89	
		T-MOTOR 13*4.4CF	50%	4.3	64	560	4800	8.80	44
			65%	5.8	86	700	5300	8.15	
			75%	7.2	107	800	5800	7.51	
			85%	9.7	144	1050	6500	7.31	
			100%	11.5	170	1200	6900	7.05	
		T-MOTOR 14*4.8CF	50%	5	74	730	4250	9.86	46
			65%	7.3	108	940	4900	8.70	
			75%	10.1	149	1200	5500	8.03	
			85%	13.5	200	1450	6050	7.26	
			100%	16.5	244	1700	6500	6.96	
	22.2	T-MOTOR 11*3.7CF	50%	5.9	131	820	7500	6.26	46
			65%	7.7	171	970	8300	5.67	
			75%	9.1	202	1130	8700	5.59	
			85%	12.2	271	1400	9750	5.17	
			100%	14.5	322	1560	10400	4.85	
		T-MOTOR 12*4CF	50%	7	155	970	6900	6.24	47
			65%	9.1	202	1160	7650	5.74	
			75%	11.8	262	1410	8500	5.38	
			85%	15.8	351	1760	9400	5.02	
			100%	28.8	639	2000	10000	3.13	

Notes: The test condition of temperature is motor surface temperature in 100% throttle while the motor run 10 min.

For the model simulation, physical parameters are needed. These parameters are shown in Table 4. The above values are stated for a single winding with DC motors, and are the phase values for a BLDC motor.

Table 4 – Physical parameters of motor.

Parameters	Symbol	Units
Motor voltage constant	Ke	volts-sec/rad
Motor torque constant	KT	N-m/amp
Motor resistance	R	ohms
Motor inductance	L	Henries
Total inertia	J	N-m-sec^2

Determination of the motor parameter

The values for reference of the motor parameters given in the motor specifications, usually provided by the manufacturer, are not very accurate, especially for the cheaper DC motors which tend to have relatively larger tolerances in their electrical and mechanical parameters. The reference [1] suggests an algebraic approach that can be applied to the determination of the motor parameters.

The process of measuring the parameter of Dc motor is described in [31]. It involves the determination of the motor resistance R, the voltage constant Ke, the torque constant KT, the motor inertia Jm, the inductance L.

The motor Kv is given by the manufacturer to be 550 RPM/V

$$\frac{i}{Kv}\frac{1}{550}\quad\frac{V}{RPM}K_e = = = 0.001818$$

$$K_e(phase) = \frac{}{1.73}01818(0.000192) = 2.02 * 10{-}_7\frac{}{RPM}v_2 \qquad [1]$$

$$K_T = \frac{k_e}{0.00684} = 0.26579\frac{lb-in}{Amp} = 0.03\frac{Nm}{Amp}$$

The inductance L was determined as shown:

$$impedance = \frac{0.1975}{0.00035} = 5642.9\ oh_{ms}$$

$$reactance = \sqrt{imp^2 - res^2} = 5642.8\ oh_{ms}$$

$$Imductance = \frac{5642.8}{2\pi * 120}\ 7.48_{Henries}$$

However, The inertia could not be measured without the Stripchart recorder.

Mathematical Model of the DC motor

DC motors have high application in industrial control system because they are easy to control and to model. The goal in the development of the mathematical model is to relate the voltage applied to the armature to the velocity of the motor. Two balance equations can be developed by considering the electrical and mechanical characteristics of the system. The equivalence circuit of a DC motor is illustrated in Figure 7.

It can be represented by a voltage source (V) across the coil of the armature. The electrical equivalence of the armature coil can be described by the inductance (L) in series with a resistance (R) and with an induced voltage (V) which opposes the voltage source.

Mechanical Characteristics

The Newton second law applied to rotor can be stated as:

$$T_e - T_w = J\frac{d^2\theta}{dt^2} \tag{15}$$

where T_e *is the electromagnetic torque*

T_w *is the torque due to rotational accelaration* j

is the moment of inertia

$$T_e = K_t I$$

$$T_w = b\theta$$

From equation (1), it is derived

$$K_t I - b\theta = J\frac{d^2\theta}{dt^2} \tag{16}$$

Electrical characteristics

A differential equation for the equivalent circuit can be derived by using Kirchoff's voltage law around the electrical loop. That is the sum of all voltages around a loop is equal to zero. The voltage across the resistor is: Ri

The voltage across the inductor is given by: $L\frac{di}{dt}$

The back Emf can be written as: $k_e\frac{d\theta}{dt}$

The Kirchoff's law can be written:

$$L\frac{di}{dt} = -Ri + V - k_e\frac{d\theta}{dt} \tag{17}$$

From equation (2) and (3), the following system can be derived

$$1 \qquad d^2\theta$$

$$J\,(K_t I - b\theta) = \frac{d^2}{dt^2}$$

$$\frac{di}{dt} = L\left(-Ri + V - k_e \frac{d\theta}{dt}\right)$$

A Simulink model can be derived [3]. This model has as input the voltage and as output the velocity of the motor shaft.

With this model, a speed profile can be defined. However to be able to relate each fly sequence to the energy available, a power profile is necessary with as input a voltage and as output each flying sequence. That is a model describing each flying phase: the takeoff, the hovering, and the landing mode. To be able to describe such model, a Simulink/SimMechanics model is used.

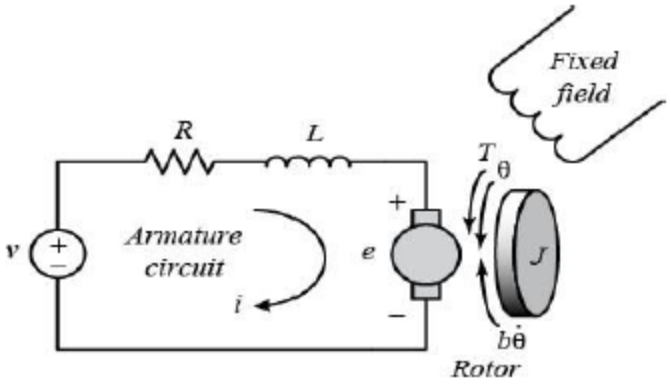

Fig. 6 - DC motor equivalence circuit

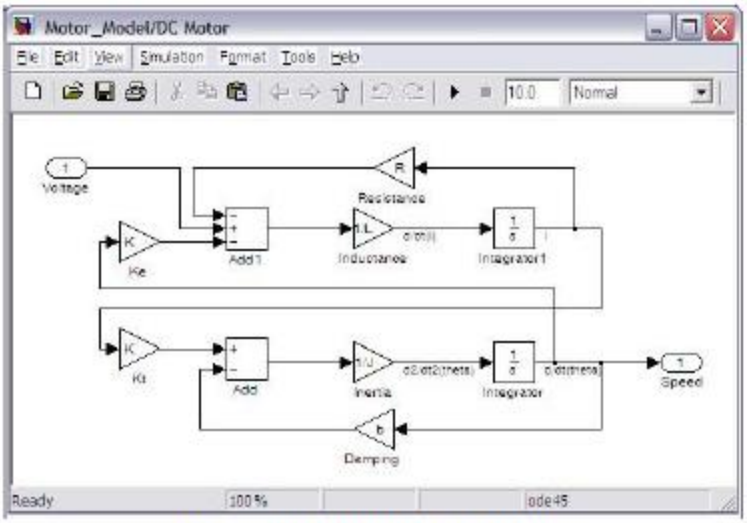

Fig. 7 – Simulink model of the motor.

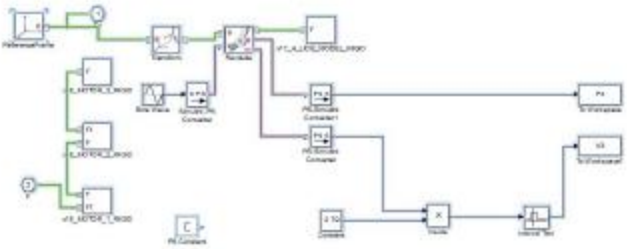

Fig. 8 – Sim Mechanics model 1

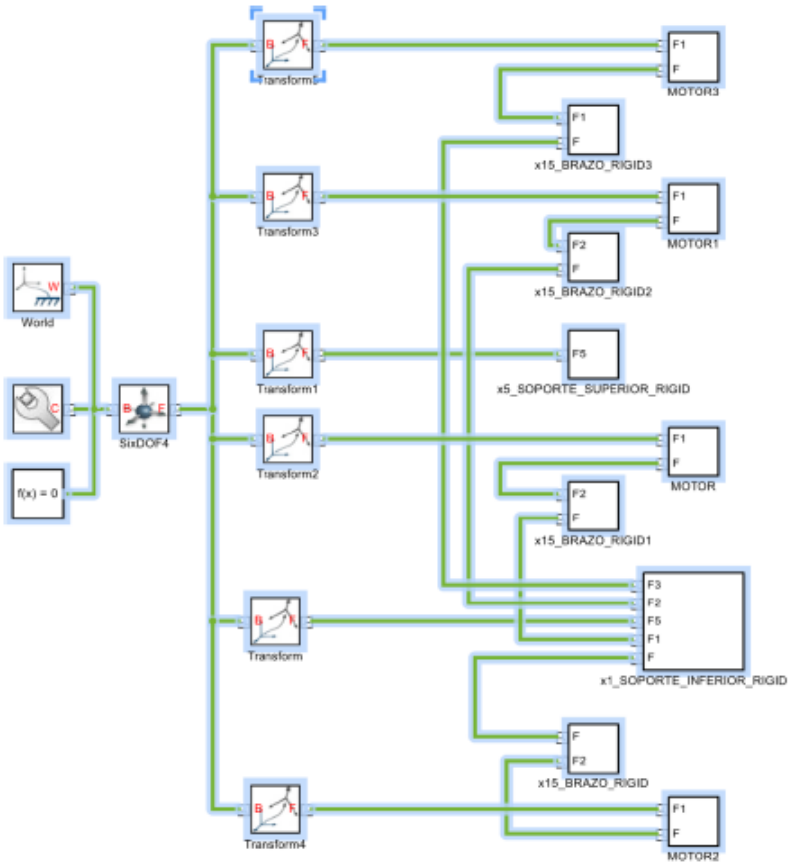

Fig. 9 – Sim Mechanics model 2

Quadcopter Modeling and Results

The PEMFC is modeled as the unique source of energy to power the quadcopter, while the four motors that run the propeller of the quadcopter are modeled as primary power sink. The block diagrams of PEMFC and motors designed in Simulink are shown in Figures 10 and 11. The results obtained from the model is shown in Figures 12 and 13.

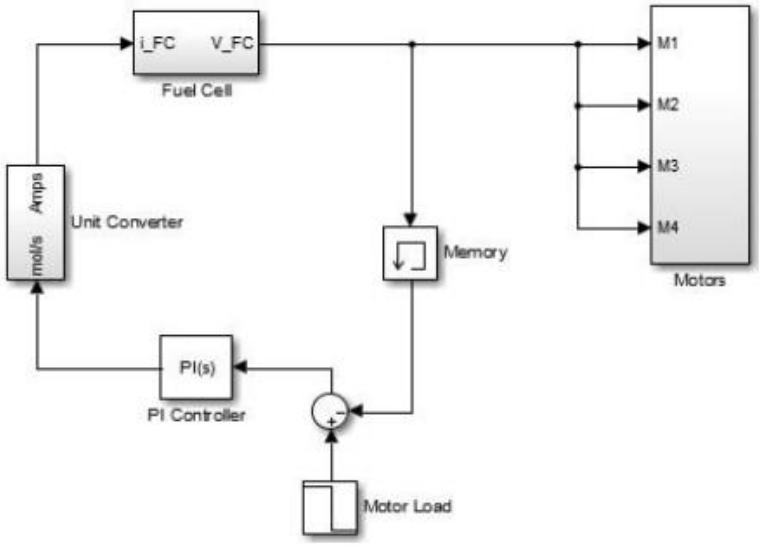

Fig. 10 – PEMFC block diagram with PID integrated with motors.

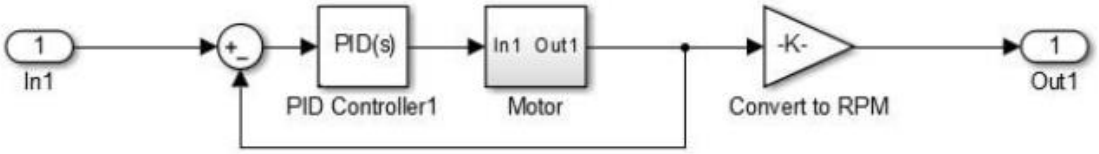

Fig. 11 – Individual motor integrated with PID control.

The combined simulation results of both PEMFC and motors with their controls incorporated are shown in figures 12 and 13. The Y-axis indicates motor speed in revolution per minute (RPM) while the X-axis represents time in seconds.

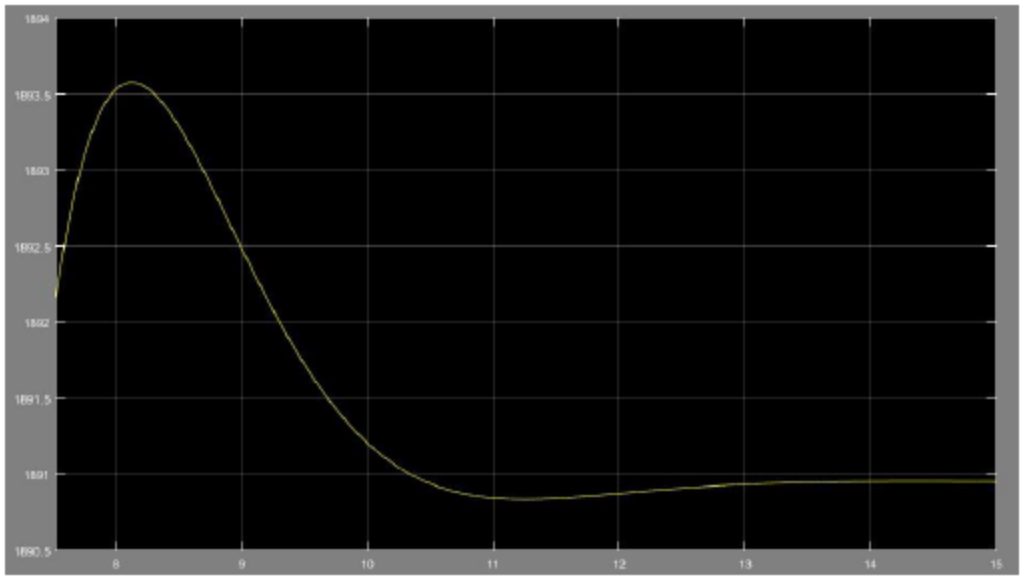

Fig. 12 – RPM of motor without PID.

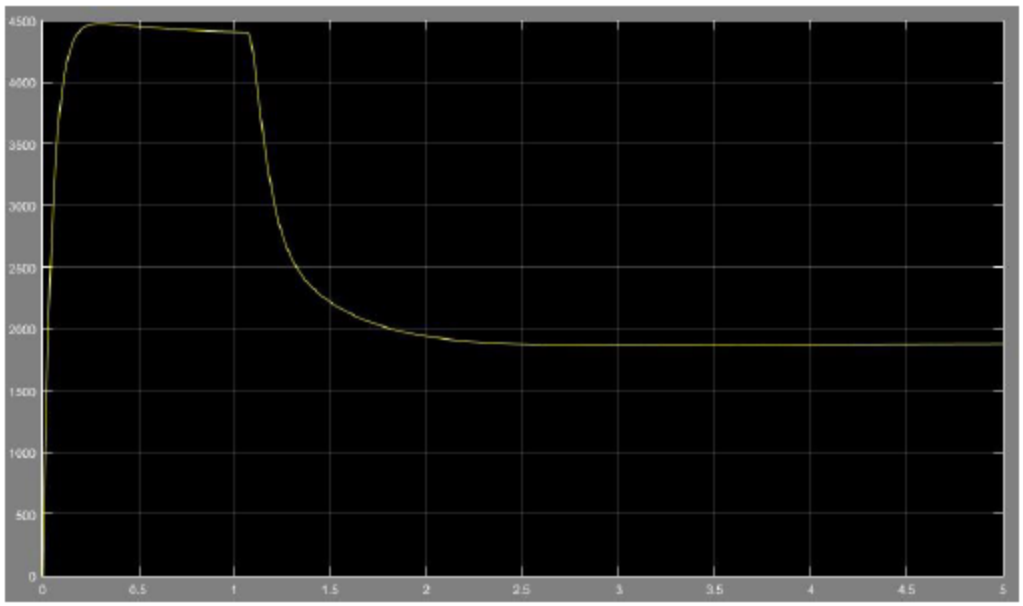

Fig. 13 – RPM of motor with PID control.

Discussion

The motor speed without a controller (Fig. 12) shows a tremendous amount of rise time, a slight overshoot, and the peak RPM is a lot less than predicted. After incorporating the PID controller, the peak RPM is slightly improved, but still less than ideal. This may be due to certain incorrect choices of motor parameters, such as the electromotive force constant (K_e). Overall, this general curve of the motor speed is expected by analyzing V_{FC} from Fig. 4. In Fig. 4, V_{FC} peaks at 0 to 1 second of the simulation. This leads to a peak in RPM from 0 to 1 second, shown in Fig. 13. Then as the voltage drops, so should the RPM drop, also demonstrated in Fig. 13. Nonetheless, both graphs from figures 4 and 13 show a matching rise-time. From Fig. 13, initially the motor starts from 0 RPM reason being it was at steady state before the input voltage. At steady state (20 V), the motor speed is approximately 1900 RPM.

Conclusion

In this study, a control-oriented PEMFC power system model is constructed and used to power a quadcopter. The output of the PEMFC is stabilized by a PI controller which adjusts the flowrate of hydrogen tank. The voltage output from the PEMFC powers the motors, which is also controlled by PID. To control the hydrogen flowrate, PI controller is chosen because its high precision in comparison to PID. PID controller is used on the motors due to its fast response time, which as a result, increases the reaction rate and mobility of the quadcopter. Calculations showed that at a medium current load, the Horizon 200W PEMFC powered quadcopter slightly exceed the minimum flight duration. Experimental results from modeling the PEMFC using Simulink revealed that it's possible to power a quadcopter using just a PEMFC while having a feasible PI controller implemented in the system to stabilize the hydrogen feed. This power system control method could serve as a more efficient alternative to that of a pure batterypowered system. Further studies have shown that a hybrid PEMFC/battery DC power system, integrated with a DC/DC converter, could also serve as a more efficient power source than conventional power sources, by providing a longer-lasting flight duration that involves a more complicated power system design [31,32]. This method not only requires an extensive background knowledge on fuel cells, but also a detailed understanding on batteries because battery selection, to pair with the fuel cell, can have a significant effect on the overall system performance [32]. Furthermore, a PEMFC/battery hybrid power system configuration and control method can be integrated with other renewable energy sources. Specifically, photovoltaic cells such as dye-sensitized solar panels, to increase mission endurance and reduce cost by powering/charging battery and devices mid-flight [31]. While this may seem inefficient due to the requirement of larger surface areas of solar panels, adding an array of photovoltaic cells specifically tuned

to an infrared laser's wavelength, laser can be used to charge UAS while they are in the air. A laserpowered UAS has already been flight tested by Lockheed Martin with a flight duration of more than 48 hours [38]. Inevitably, the slight overshoot of fuel cell output can be suppressed to zero with a more efficient method of tuning the PI control, as well as the fluctuations of stead-state error can be reduced by implementing a voltage stabilizers such as a DC/DC converter, as well as higher peak RPM can be achieved with a more optimized motor specification.

References

[1] Gur O, Rosen A. Optimizing electric propulsion systems for unmanned aerial vehicles. J Aircr 2009;46:1340e53.

[2] Shin Y, Chang S-H, Koo S-O. Performance test and simulation of a reciprocating engine for long endurance miniature unmanned aerial vehicles. Proc Inst Mech Eng Part D J Automob Eng 2005;219:573e81.

[3] Bradley TH, Moffitt BA, Fuller TF, Mavris DN, Parekh DE. Comparison of design methods for fuel-cell-powered unmanned aerial vehicles. J Aircr 2009;46:1945e56.

[4] Bradley TH, Moffitt BA, Mavris DN, Fuller TF, Parekh DE. Hardware-in-the-loop testing of a fuel cell aircraft powerplant. J Propul Power 2009;25:1336e44.

[5] Kim T, Kwon S. Design and development of a fuel cellpowered small unmanned aircraft. Int J Hydrogen Energy 2012;37:615e22.

[6] Kim K, Kim T, Lee K, Kwon S. Fuel cell system with sodium borohydride as hydrogen source for unmanned aerial vehicles. J Power Sources 2011;196:9069e75.

[7] Bradley TH, Moffitt BA, Mavris DN, Parekh DE. Development and experimental characterization of a fuel cell powered aircraft. J Power Sources 2007;171:793e801.

[8] Rhoads G, Bradley T, Wagner N, Taylor B, Keen D. Design and flight test results for a 24 hour fuel cell unmanned aerial vehicle, Paper AIAA-2010-6690. In: 8th annual international energy conversion engineering conference (IECEC). American Institute of Aeronautics and Astronautics; 2010.

[9] Chiang C, Herwerth C, Mirmirani M, Ko A, Matsuyama S, Choi SB, et al. Systems integration of a hybrid PEM fuel cell/ battery powered endurance UAV, Paper AIAA-2008-0151. In: 46th AIAA aerospace sciences meeting and exhibit. American Institute of Aeronautics and Astronautics; 2008.